Available online at www.sciencedirect.com
ScienceDirect
Trans. Nonferrous Met. Soc. China 22(2012) 2171−2178
Transactions of Nonferrous Metals Society of China
www.tnmsc.cn

Microstructure and tribological properties of laser cladding Fe-based coating on pure Ti substrate

CHEN Jian-min[1], GUO Chun[2], ZHOU Jian-song[1]

1. State Key Laboratory of Solid Lubrication, Lanzhou Institute of Chemical Physics, Chinese Academy of Sciences, Lanzhou 730000, China;
2. Luoyang Ship Material Research Institute, Luoyang 471039, China

Received 29 September 2011; accepted 30 April 2012

Abstract: Fe-based coating was produced on pure Ti substrate by the laser cladding technology. The composition and microstructure of the fabricated coating were analyzed by scanning electron microscopy (SEM), X-ray diffraction (XRD) and transmission electron microscopy (TEM) technique. The tribological properties were tested through sliding against AISI52100 steel ball at different normal loads and sliding speeds. Besides, the morphologies of the worn surfaces and wear debris were analyzed by scanning electron microscopy (SEM) and three dimensional (3D) non-contact surface mapping. The results show that the prepared Fe-based coating has a high hardness of about 860 $HV_{0.2}$ and exhibits an average wear rate of $(0.70-2.32)\times10^{-6}$ $mm^3/(N\cdot m)$, showing that the Fe-based coating can greatly improve the wear resistance of pure Ti substrate. The wear mechanism of the coating involves moderate adhesive and abrasive wear.

Key words: titanium; Fe-based coating; laser cladding; wear

1 Introduction

Titanium and its alloys have high strength, excellent corrosion resistance, low density, high specific strength, low modulus and good biocompatibility, so they are vastly expanded into many industrial applications such as aeronautical, marine, power generation, chemical industries, sports and leisure transportation, and biomedical devices [1−10]. However, their poor wear resistance is a serious concern for applications where wear phenomena are present, which limits their engineering applications [11−18]. Therefore, there is an increasing interest in improving surface properties of titanium and its alloys through various surface modification techniques, i.e., laser cladding, ion implantation, electroless deposition, physical vapor deposition (PVD), chemical vapor deposition (CVD), carburizing, nitriding, and oxidation studied [19−26]. More recently, laser cladding technology has attracted attention of various research groups due to several unique advantages such as laser cladding with high energy density, offering high heating/cooling rates (10^3–10^8 K /s) for the development of non-equilibrium phases with fine grained microstructure and novel properties [27], and also the fabricated coatings are very dense and have strong metallurgical bonding to substrates [28].

Laser cladding Fe-based coatings are regarded as promising materials for tribological applications due to their high bonding strength, high hardness and excellent wear resistance, as well as cheaper than cobalt- or nickel-based coatings [29−33]. So, it is anticipated that Fe-based coatings can be prepared on titanium and its alloys' surface with excellent wear resistance property, and can be used as a candidate material to aid to the surface engineering titanium and its alloys components working under wear conditions. However, to the best of our knowledge, there are few data on the tribological characteristics of laser cladding Fe-based coating prepared on titanium and its alloys.

Therefore, in the present study, to improve the wear resistance of pure Ti substrate, Fe-based coating was fabricated on its surface by laser cladding technology. The

Foundation item: Project (51045004) supported by the National Natural Science Foundation of China; Project (2006AA03A219) supported by Hi-tech Research and Development Program of China; Project (YYYJ-0913) supported by Knowledge Innovation Project in Chinese Academy of Sciences

Corresponding author: CHEN Jian-min; Tel: +86-931-4968018; Fax: +86-931-8277088; E-mail: chenjm@lzb.ac.cn

DOI: 10.1016/S1003-6326(11)61445-3

microstructure and tribological properties of the prepared Fe-based coating were systematically investigated.

2 Experimental

Pure Ti (TA2) discs with 31 mm in diameter, 10 mm in thickness were used as the substrates. Prior to coating preparation, the substrates were abraded with SiO_2 grit. The Fe-based alloy powder $Fe_{62}Ni_3Cr_4Mo_2W_3Si_6B_{17}C_3$ (in mole fraction) was used as the starting material. The powder was pre-placed onto the surface of the substrate without any binding materials, with a thickness of approximately 1.0 mm before laser cladding.

A 10 kW CO_2 laser processing system was performed for laser cladding. Laser processing was conducted in argon shielding gas. The laser beam was focused down to a diameter of 3 mm. Coverage was achieved with overlapped track of 50%. The other laser processing parameters were as follows: laser power 2 kW, beam traverse speed 1000 mm/min.

After laser cladding the Fe-based coating was sectioned and ground for the microstructural analysis. Metallographic cross section of the laser cladding sample was ground with 600, 1200 and 2000# SiC sandpapers, and a 1.0 μm Cr_2O_3 paste. The sample was then etched in a solution of HF, HNO_3 and H_2O with a volume ratio of 2:1:47 at room temperature for approximately 60 s before observation by a scanning electron microscope (SEM) (JSM−5600LV; JEOL, Ltd.) equipped with energy-dispersive spectrometer (EDS, KEVEX). A TECNAI-G^2-F30 field emission transmission electron microscope (TEM, FEI, Oregon, USA), operating at 300 kV, was performed to obtain TEM images. The phase compositions of the composite coating were identified with X-ray diffraction (XRD) analysis (D/max 2400; Rigaku, Ltd.) using 40 kV, 100 mA and Cu K_α radiation in a scanning range of 2θ from 15° to 85°.

The microhardness of Fe-based coating along the depth direction was analyzed on a microhardness tester (MH−5 Vickers; Shanghai Everone Instrument, Ltd.) at 1.96 N for a dwelling time of 5 s.

The tribilogical behaviors of the laser cladding Fe-based coating were evaluated on a reciprocating tribometer (UMT−2MT; Center for Tribology, Inc.) sliding against a 6 mm diameter AISI52100 steel ball (with a hardness of about 700 $HV_{0.2}$) in a nominally dry environment, at normal loads from 5 to 15 N at a sliding speed of 0.1 m/s. Tests with sliding speeds from 0.025 to 0.200 m/s at a normal of 10 N were also conducted. The amplitude was 5 mm and total sliding distance was 180 m for each test. The friction coefficient was continuously recorded by the test system and the wear volume was determined using a three-dimensional (3D) non-contact surface mapping profiler (MicroXAM; ADE Corporation, Inc.). Three tests were conducted under each test condition, and the averaged values were used. The worn surfaces were also analyzed using a SEM and surface mapping profiler.

3 Results and discussion

3.1 Composition and microstructure of Fe-based coating

Figure 1 presents XRD patterns of the laser cladding coating. It can be found from Fig. 1 that the prepared coating is mainly composed of Fe, Fe_2Ti, Fe_2B, Fe_3Si, Ti_2Ni and Fe_2O_3 phases. After laser cladding, Fe element partly reacted with the melt Ti to transform to Fe_2Ti intermetallic compound, which could be attributed to the high energy density of the CO_2 laser beam. In addition, the existence of Fe_2O_3 phase in the laser cladding coating can be attributed to the reaction between melt Fe and residual air in the protector during laser cladding.

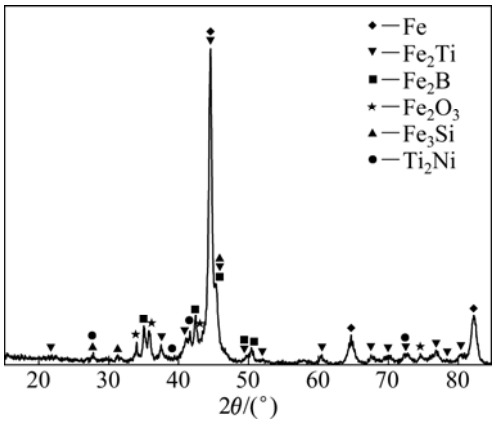

Fig. 1 XRD pattern of laser cladding coating

Figure 2 shows the SEM image and corresponding elements Fe and Ti distribution map on cross section of the coating. It can be seen that the prepared coating is free of cracks. However, few pores are visible in coating zone, which could be explained by the gas trapping due to large fluid viscosity induced by material particles in the laser melt pool [34] or the encapsulated bubbles generated during the laser cladding process [35]. In addition, it can be observed from Fig. 2 that the prepared Fe-based coating is metallurgically bonded to its substrate with a thickness of about 1.0 mm. Furthermore, it can be also seen that the corresponding Fe element is dispersed relatively uniformly on the cross section of coating, and Ti element with relatively more content near the coating/substrate interface. It should be noticed that between coating and substrate, the coating has a diffuse zone with depth of about 60 μm. This is a favorable evidence for Fe-based coating to be metallurgically

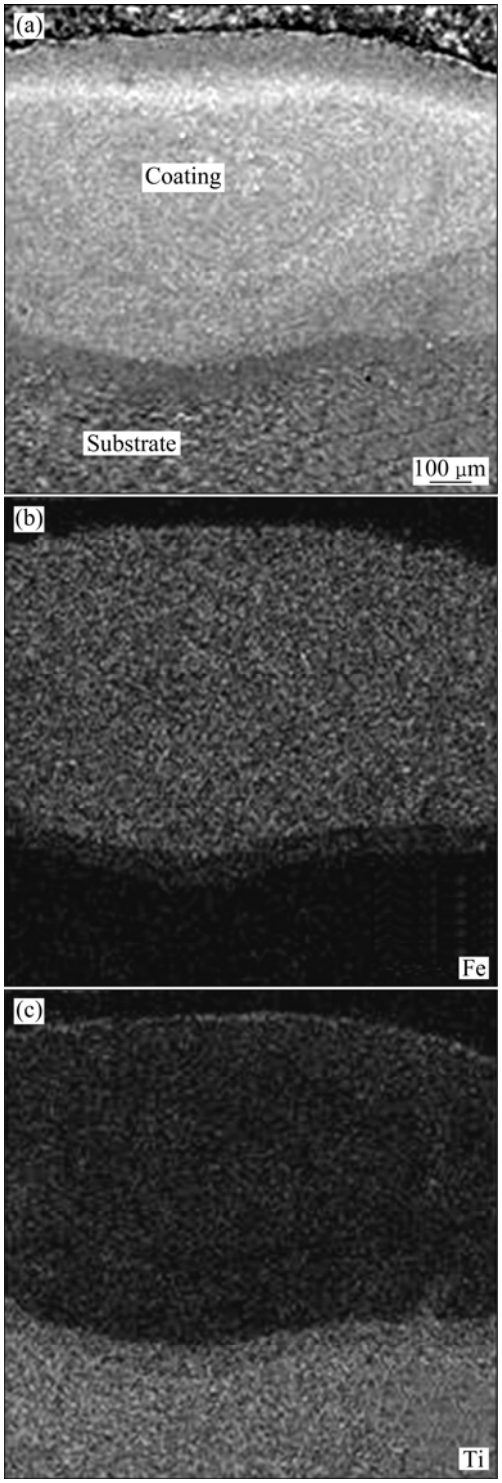

Fig. 2 SEM image (a) and corresponding elements Fe (b) and Ti (c) distribution map on cross section of Fe-based coating

bonded to the substrate.

Figure 3 gives the cross-sectional SEM micrograph of laser cladding Fe-based coating, with image near the top surface and the interface presented for better observing the interfacial microstructure. As shown in Fig. 3(b), it is further confirmed that the prepared Fe-based coating was metallurgically bonded to the pure Ti substrate. The Fe-based coating was composed of fine block-like phase near the top surface and bottom with a size almost less than 5 μm, which is attributed to the fact that laser cladding process offers high heating and cooling rates (10^3−10^8 K /s) for the development of fine grained microstructure [27].

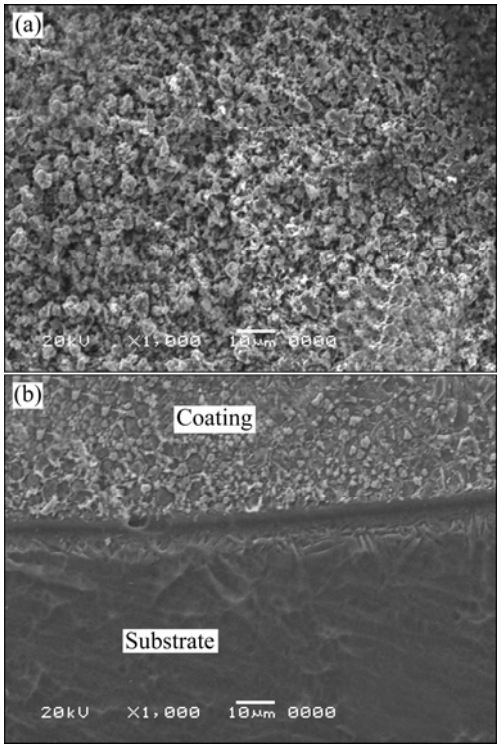

Fig. 3 Cross-sectional SEM micrographs of Fe-based coating near to top surface (a) and near to interface (b)

Detailed microstructural characterization of the Fe-based coating was analyzed by TEM, which is shown in Fig. 4. The bright field TEM image indicates that Fe-based coating consists of block-like grains, and the corresponding SAED pattern clearly reveals that it contains heteromorphy Fe_2Ti phase.

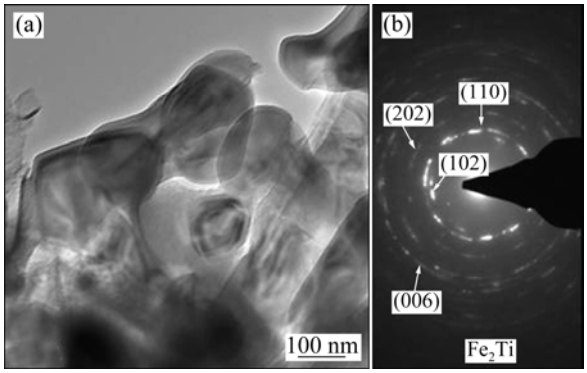

Fig. 4 TEM image (a) and corresponding SAED pattern (b) of Fe-based coating

3.2 Microhardness of Fe-based coating

Figure 5 gives the microhardness profile along the

depth direction of laser cladding Fe-based coating. It can be seen that Fe-based coating gives a high average hardness of approximately 860 $HV_{0.2}$, which is about 4.5 times that of pure Ti substrate (approximately 190 $HV_{0.2}$). The distinctive high hardness of the Fe-based coating could be attributed to the presence of hard phases, such as Fe_2Ti, Fe_2B, Fe_3Si and Ti_2Ni phases, in the coating zone. It is also clear that the microhardness profile of Fe-based coating in the coating/substrate bonding zone has a sharp falling. Namely, the microhardness greatly varied from about 780 $HV_{0.2}$ to 300 $HV_{0.2}$.

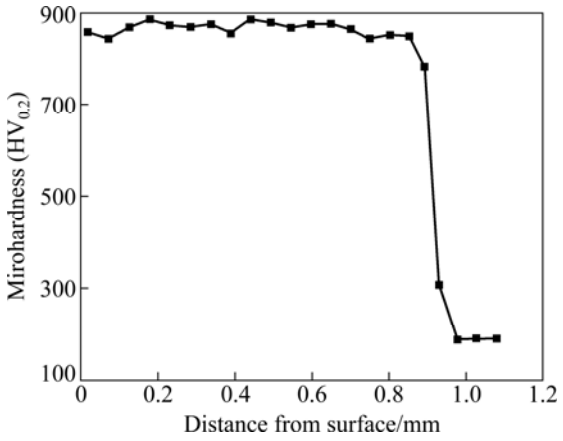

Fig. 5 Microhardness profile of Fe-based coating

3.3 Tribological properties of Fe-based coating at different normal loads and sliding speeds

Figures 6 and 7 show the variations of friction coefficient of the laser cladding Fe-based coating as a function of normal load (at a sliding speed of 0.1 m/s) and sliding speed (at a normal load of 10 N), respectively. It is obviously seen that the friction coefficients of Fe-based coating decreased with increasing normal load or sliding speed. The friction coefficients of Fe-based coating decreasing with increasing normal load can be explained by the normal load increasing faster than the increase of apparent contact area. Due to the fact that Fe-based coating has significantly high microhardness and leads to high loading capacity, during the friction and wear tests the Fe-based coating sliding against AISI52100 steel ball presented a relatively small increase rate in the apparent contact area and corresponding lower friction coefficients at high normal loads [36]. The friction coefficients of Fe-based coating decreased with increasing sliding speed due to higher sliding speeds under unlubricated dry sliding conditions; contact shearing and ploughing was so rapid that friction heat was generated at a rate much faster than that being conducted away, which results in generation of much more frictional heat, accordingly high temperature elevation on the contact surface. As a result, with increasing the sliding speed, the local temperature increased [37,38]. The more intense localized heat lowered the strength of the contact surfaces more greatly and formed tribolayers, thereby lowering the friction coefficient rapidly [39].

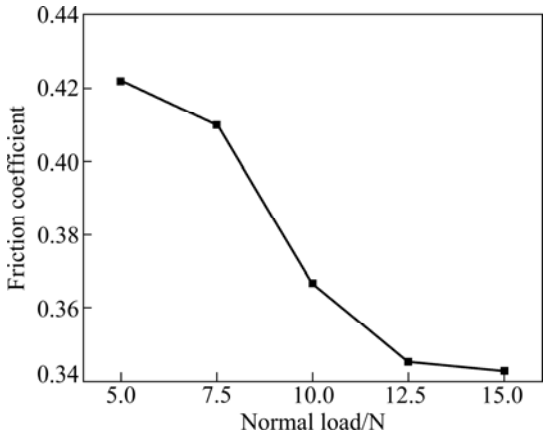

Fig. 6 Variation of friction coefficient of Fe-based coating against AISI−52100 steel ball as function of normal load at given sliding speed of 0.1 m/s

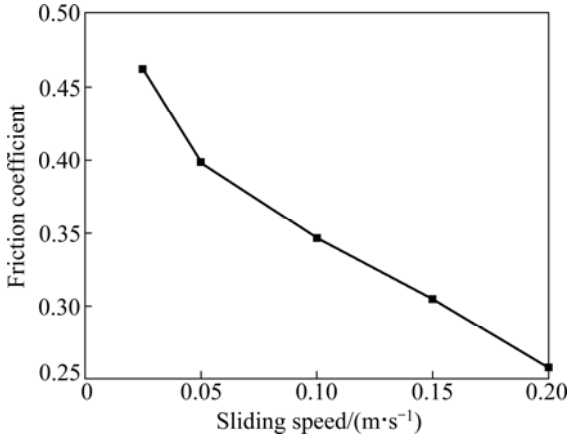

Fig. 7 Variation of friction coefficient of Fe-based coating against AISI−52100 steel ball as function of sliding speed at given normal load 10 N

The variations of wear rate of the laser cladding Fe-based coating as a function of normal load (at a sliding speed of 0.1 m/s) and sliding speed (at a normal load of 10 N) are presented in Fig. 8 and Fig. 9, respectively. As can be seen in Fig. 8, the wear rate of the Fe-based coating increased with increasing the normal load, which is in accordance with the Archard's wear law [40]. While the wear rate of the coating decreased rapidly with increasing the sliding speed. The wear rate of Fe-based coating decreased with increasing the sliding speed, which is attributed to the fact that at higher sliding speeds, ploughing and shearing was so rapid that friction heat was generated at a rate much faster than that being conducted away. Thus, with increasing the sliding speed, the temperature of contact

area increased, and the high temperature lowered the strength of the contact surfaces, thereby lowering the friction coefficient, and leading to reducing in wear rate. In addition, it is interesting to notice that the wear rate of the coating under these wear conditions exhibited average wear rate of $(0.70-2.32)\times10^{-6}$ mm^3/(N·m). It has been found in our previous work that the wear rate of pure Ti substrate in the 10^{-4} mm^3/(N·m) order of magnitude [41]. This result indicates that the laser cladding Fe-based coating has an excellent wear resistance and can greatly improve the wear resistance of pure Ti substrate.

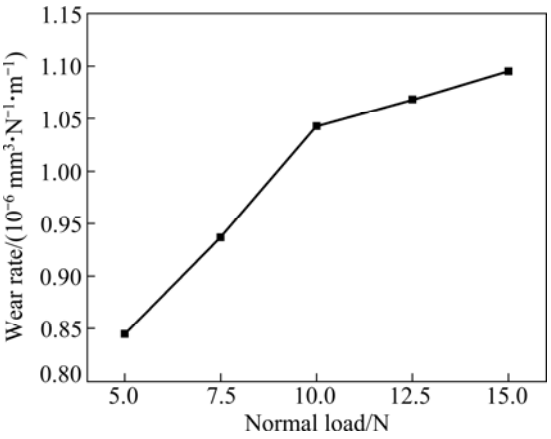

Fig. 8 Variation of wear rate of Fe-based coating against AISI−52100 steel ball as function of normal load at given sliding speed of 0.1 m/s

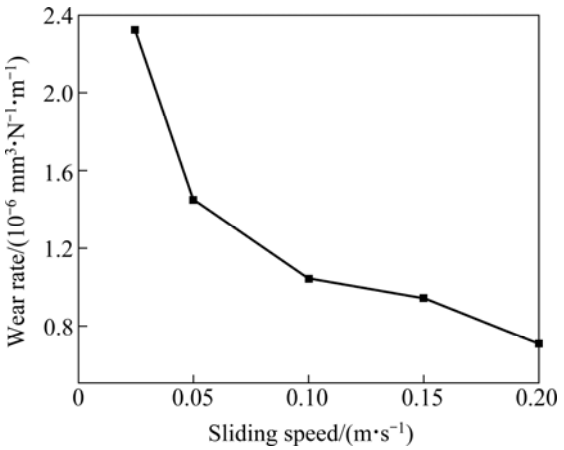

Fig. 9 Variation of wear rate of Fe-based coating against AISI−52100 steel ball as function of sliding speed at given normal load of 10 N

To understand the underlying wear mechanism of laser cladding Fe-based coating upon the variation of normal load and sliding speed, SEM images of the worn surfaces of the coatings were analyzed, as shown in Fig. 10. It can be seen that shallow grooves and tribolayers (patches) emerged on the worn surfaces of the Fe-based coating (see Fig. 10). This fact indicates the abrasive and adhesive wear occurred during the wear tests

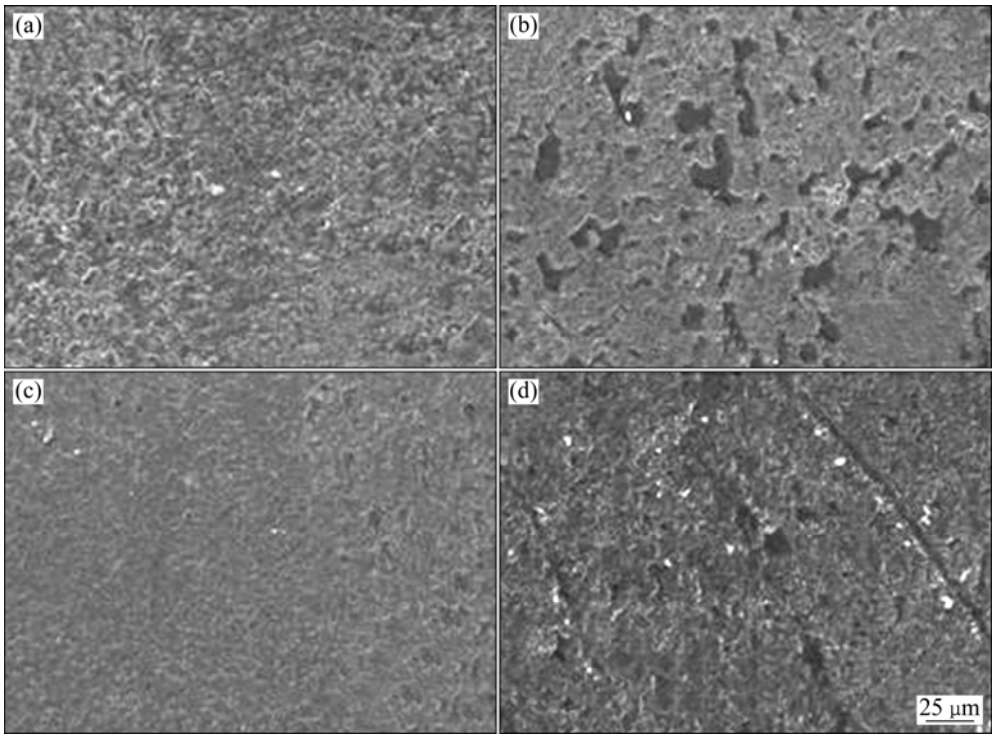

Fig. 10 SEM images of worn surfaces on Fe-based coatings under different conditions: (a) Normal load of 5 N, sliding speed of 0.1 m/s; (b) Normal load of 15 N, sliding speed of 0.1 m/s; (c) Normal load of 10 N, sliding speed of 0.025 m/s; (d) Normal load of 10 N, sliding speed of 0.2 m/s

for Fe-based coating and AISI52100 steel ball friction pairs. It should be noted that with the increase in normal load from 5 N to 15 N and sliding speed from 0.025 m/s to 0.2 m/s, tribolayers are developed on the worn surface of Fe-based coating (see Fig. 10), namely, increasing the normal load and sliding speed increases the possibility of formation of tribolayer. It is known that local temperature increases with the increase of normal load and sliding speed [42], and dry sliding wear causes large plastic strain, contact shearing and ploughing, leading to relatively high temperature on the worn surface of friction pair. Furthermore, the high local temperature may cause the transfer of elements and the tribolayers may form. The tribolayer can prevent direct contact between the frictional pair, reducing the contact area, thereby the friction coefficient drastically decreases [37−39,43].

In order to better understand the underlying wear mechanism, the counterbody AISI52100 steel ball and the wear debris were also analyzed. Figure 11 gives the 3D non-contact surface mapping of the worn surface of the AISI52100 steel ball at normal loads of 5 N and 15 N (sliding speed of 0.1 m/s) and at sliding speeds of 0.025 m/s and 0.2 m/s (normal load of 10 N). As can be seen from the four figures that the worn surface of the AISI52100 steel ball shows regular grooves. This result confirms the existence of abrasive wear between the friction pair. And it can be also observed that at a given sliding speed of 0.1 m/s, the diameter of wear scar of the AISI52100 steel ball increased with increasing normal load (see Fig. 11(a) and Fig. 11(b)), while the diameter of the AISI52100 steel ball decreased with increasing the sliding speed from 0.05 m/s to 0.2 m/s at a given normal of 10 N (see Fig. 11(c) and Fig. 11(d)). This is in good agreement with the result of the wear rates of the Fe-based coating at different normal loads and sliding speeds. Figure 12 shows the SEM images of the wear debris of the Fe-based coating against AISI52100 steel ball at a normal load of 15 N (sliding speed of 0.1 m/s). The wear debris is block-like and in spherical shape with a small size. The generation of small wear debris during the wear testing indicates that the friction pair experienced moderate wear and the Fe-based coating has an excellent wear resistance [3]. The spherical shaped wear debris shown in Fig. 12 is formed from the block-like wear debris through milling [44].

4 Conclusions

1) Fe-based coating was fabricated successfully on pure Ti substrate by laser cladding.

2) It was found that the prepared coating mainly contains Fe, Fe_2Ti, Fe_2B, Fe_3Si, Ti_2Ni and Fe_2O_3 phases. The prepared Fe-based coating was metallurgically bonded to the pure Ti substrate and composed of fine block-like phase near the top surface and bottom with a size less than 5 μm.

3) The Fe-based coating has a high average microhardness of about 860 $HV_{0.2}$ in the coating zone. The friction and wear experiments show that Fe-based coating with average wear rate of $(0.70−2.32)\times10^{-6}$ $mm^3/(N\cdot m)$ can greatly improve the wear resistance of pure Ti substrate, experiencing moderate adhesive and abrasive wear.

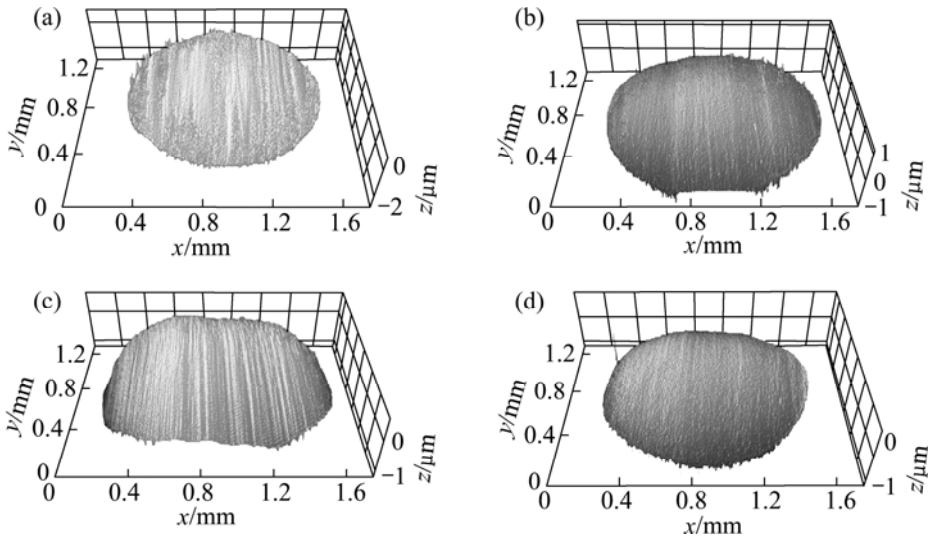

Fig. 11 3D non-contact surface mapping of worn surfaces of counterbody AISI52100 steel ball: (a) Normal load of 5 N, sliding speed of 0.1 m/s; (b) Normal load of 15 N, sliding speed of 0.1 m/s; (c) Normal load of 10 N, sliding speed of 0.025 m/s; (d) Normal load of 10 N, sliding speed of 0.2 m/s

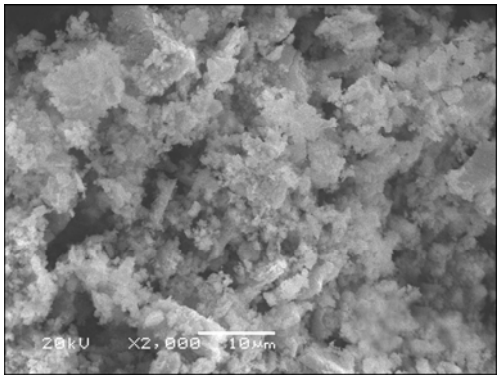

Fig. 12 SEM image of wear debris of Fe-based coating against AISI52100 steel ball at normal load of 15 N and sliding speed of 0.1 m/s

References

[1] VOJTECH D, NOVAK P, MACHAC P, MORT'ANIKOVA A, JUREK K. Surface protection of titanium by Ti_5Si_3 silicide layer prepared by combination of vapour phase siliconizing and heat treatment [J]. Journal of Alloys and Compounds, 2008, 464: 179−184.

[2] VREELING J A, OCEL K V, de HOSSON J T M. Ti−6Al−4V strengthened by laser melt injection of WCp particles [J]. Acta Materialia, 2002, 50: 4913−4924.

[3] GUO B, ZHOU J, ZHANG S, ZHOU H, PU Y, CHEN J. Tribological properties of titanium aluminides coatings produced on pure Ti by laser surface alloying [J]. Surface and Coatings Technology, 2008, 202: 4121−4129.

[4] ZHENG M, FAN D, LI X K, ZHANG J B, LIU Q B. Microstructure and in vitro bioactivity of laser-cladded bioceramic coating on titanium alloy in a simulated body fluid [J]. Journal of Alloys and Compounds, 2010, 489: 211−214.

[5] PEI C, FAN Q, CAI H, LI J. High temperature deformation behavior of the TC6 titanium alloy under the uniform DC electric field [J]. Journal of Alloys and Compounds, 2010, 489: 401−407.

[6] VOJTECH D, CIZOVA H, JUREK K, MAIXNER J. Influence of silicon on high-temperature cyclic oxidation behaviour of titanium [J]. Journal of Alloys and Compounds, 2005, 394: 240−249.

[7] XU Chun, ZHU Wen-feng. Transformation mechanism and mechanical properties of commercially pure titanium [J]. Transactions of Nonferrous Metals Society of China, 2010, 20: 2162−2167.

[8] CHEN Yong-nan, WEI Jian-feng, ZHAO Yong-qing, ZHENG Jing. Microstructure evolution and grain growth behavior of Ti14 alloy during semi-solid isothermal process [J]. Transactions of Nonferrous Metals Society of China, 2011, 21: 1018−1022.

[9] ZHOU Zhong-bo, FEI Yue, LAI Min-jie, KOU Hong-chao, CHANG Hai, SHANG Guo-qiang, ZHU Zhi-shou, LI Jin-shan, ZHOU Lian. Microstructure and mechanical properties of new metastable beta type titanium alloy [J]. Transactions of Nonferrous Metals Society of China, 2010, 20: 2253−2258.

[10] LIU Hui-jie, FENG Xiu-li. Microstructures and interfacial quality of diffusion bonded TC21 titanium alloy joints [J]. Transactions of Nonferrous Metals Society of China, 2011, 21: 58−64.

[11] TSUJI N, TANAKA S, TAKASUGI T. Evaluation of surface-modified Ti−6Al−4V alloy by combination of plasma-carburizing and deep-rolling [J]. Materials Science and Engineering A, 2008, 488: 139−145.

[12] GARCIA I, DAMBORENEA J J D. Corrosion properties of TiN prepared by laser gas alloying of Ti and Ti6Al4V [J]. Corrosion Science, 1998, 40: 1411−1419.

[13] BAKER T N, SELAMAT M S. Surface engineering of Ti−6Al−4V by nitridingand powder alloying using CW CO_2 laser [J]. Materials Science and Technology, 2008, 24: 189−200.

[14] LIU Yong, YANG De-zhuang, HE Shi-yu, WU Wan-liang. Dry sliding wear of Ti−6Al−4V alloy in air and vacuum [J]. Transactions of Nonferrous Metals Society of China, 2003, 13: 1137−1140.

[15] YU Zhen-tao, ZHENG Yu-feng, NIU Jin-ling, HUANGFU Qiang, ZHANG Ya-feng, YU Sen. Microstructure and wear resistance of Ti−3Zr−2Sn−3Mo−15Nb (TLM) alloy [J]. Transactions of Nonferrous Metals Society of China, 2007, 17(3): s495−s499.

[16] WU Wan-liang, ZHANG Ying-chun, LI Xue-wei, SUN Jian-feng. Laser cladding of Ti−6Al−4V titanium alloy with Ti + TiC powders [J]. Transactions of Nonferrous Metals Society of China, 2005, 15(s3): 430−433.

[17] REN Yu, TAN Cheng-wen, ZHANG Jing, WANG Fu-chi. Dynamic fracture of Ti−6Al−4V alloy in Taylor impact test [J]. Transactions of Nonferrous Metals Society of China, 2011, 21: 223−235.

[18] LIN Xiu-zhou, ZHU Min-hao, ZHENG Jian-feng, LUO Jun, MO Ji-liang. Fretting wear of micro-arc oxidation coating prepared on Ti6Al4V alloy [J]. Transactions of Nonferrous Metals Society of China, 2010, 20: 537−546.

[19] DONG H, LI X Y. Oxygen boost diffusion for the deep-case hardening of titanium alloys [J]. Materials Science and Engineering A, 2000, 280: 303−310.

[20] FU Y, YAN B, LOH N L, SUN C Q, HING P. Characterization and tribological evaluation of MW-PACVD diamond coatings deposited on pure titanium [J]. Materials Science and Engineering A, 2000, 282: 38−48.

[21] YILDIZ F, YETIM A F, ALSARAN A, ÇELIK A. Plasma nitriding behavior of Ti6Al4V orthopedic alloy [J]. Surface & Coatings Technology, 2008, 202: 2471−2476.

[22] JIANG P, HE X L, LI X X, YU L G, WANG H M. Wear resistance of a laser surface alloyed Ti−6Al−4V alloy [J]. Surface and Coatings Technology, 2000, 130: 24−28.

[23] NOLAN D, HUANG S W, LESKOVSEK V, BRAUN S. Sliding wear of titanium nitride thin films deposited on Ti−6Al−4V alloy by PVD and plasma nitriding processes [J]. Surface & Coatings Technology, 2006, 200: 5698−5705.

[24] LIU Hong-xi, TANG Bao-yin, WANG Lang-ping, WANG Xiao-feng. Improvement on surface properties of titanium alloy by plasma immersion ion implantation technique [J]. Rare Metal Materials and Engineering, 2005, 34(8): 1318−1321. (in Chinese)

[25] VADIRAJ A, KAMARAJ M, GNANAMOORTHY R. Fretting wear studies on uncoated, plasma nitrided and laser nitrided biomedical titanium alloys [J]. Materials Science and Engineering A, 2007, 445−446: 446−453.

[26] MAHMOUD S S. Electroless deposition of nickel and copper on titanium substrates: Characterization and application [J]. Journal of Alloys and Compounds, 2009, 472: 595−601.

[27] DAS M, BALLA V K, BASU D, BOSE S, BANDYOPADHYAY A. Laser processing of SiC-particle-reinforced coating on titanium [J]. Scripta Materialia, 2010, 63: 438−441.

[28] NAVAS C, COLACO R, de DAMBORENEA J, VILAR R. Abrasive wear behaviour of laser clad and flame sprayed-melted NiCrBSi coatings [J]. Surface & Coatings Technology, 2006, 200: 6854−6862.

[29] WANG X, ZHANG M, QU S. Development and characterization of (Ti, Mo)C carbides reinforced Fe-based surface composite coating produced by laser cladding [J]. Optics and Lasers in Engineering, 2010, 48: 893−898.

[30] WANG X H, QU S Y, DU B S, ZOU Z D. In situ synthesised TiC particles reinforced Fe based composite coating produced by laser

cladding [J]. Materials Science and Technology, 2009, 25: 388−392.
[31] WU C, MA M, LIU W, ZHONG M, ZHANG W, ZHANG H. Laser producing Fe-based composite coatings reinforced by in situ synthesized multiple carbide particles [J]. Materials Letters, 2008, 62: 3077−3080.
[32] WU Chao-feng, MA Ming-xing, LIU Wen-jin, ZHONG Min-lin, ZHANG Hong-jun, ZHANG Wei-ming. Laser cladding in-situ carbide particle reinforced Fe-based composite coatings with rare earth oxide addition [J]. Journal of Rare Earths, 2009, 27(6): 997−1002.
[33] WANG X H, ZHANG M, DU B S, QU S Y, ZOU Z D. Microstructure and wear properties of in situ multiple carbides reinforced Fe based surface composite coating produced by laser cladding [J]. Materials Science and Technology, 2010, 26: 935−939.
[34] AMADO J M, TOBAR M J, ALVAREZ J C, LAMAS J, YANEZ A. Laser cladding of tungsten carbides (Spherotene (R)) hardfacing alloys for the mining and mineral industry [J]. Applied Surface Science, 2009, 255: 5553−5556.
[35] CHAO M J, WANG W L, LIANG E J, OUYANG D. Microstructure and wear resistance of TaC reinforced Ni-based coating by laser cladding [J]. Surface and Coatings Technology, 2008, 202: 1918−1922.
[36] ZHU Y C, YUKIMURA K, DING C X, ZHANG P Y. Tribological properties of nanostructured and conventional WC−Co coatings deposited by plasma spraying [J]. Thin Solid Films, 2001, 383: 277−282.
[37] LA P, MA J, ZHU Y T, YANG J, LIU W, XUE Q, VALIEV R Z. Dry-sliding tribological properties of ultrafine-grained Ti prepared by severe plastic deformation [J]. Acta Materialia, 2005, 53: 5167−5173.
[38] SHAFIEI A, ALPAS A. Effect of sliding speed on friction and wear behaviour of nanocrystalline nickel tested in an argon atmosphere [J]. Wear, 2008, 265: 429−438.
[39] CHU C L, WU S K. A study on the dry uni-directional sliding behaviour of tiatnium aluminides [J]. Scripta Matallet Mater, 1995, 33: 139−143.
[40] ARCHARD J F. Contact and rubbing of flat surfaces [J]. Journal of Applied Physics, 1953, 24: 981−988.
[41] GUO C, ZHOU J, ZHAO J, CHEN J. Effect of ZrB_2 on the microstructure and wear resistance of Ni-based composite coating produced on pure Ti by laser cladding [J]. Tribology Transactions, 2011, 54: 80−86.
[42] ASADIKOUHANJANI S, ZAREBIDAKI A, AKBARI A. The effect of sliding speed and amount of loading on friction and wear behavior of Cu–0.65 wt.%Cr alloy [J]. Journal of Alloys and Compounds, 2009, 486: 319−324.
[43] GUO B G, ZHOU J S, ZHANG S T, ZHOU H D, PU Y P, CHEN J M. Tribological properties of titanium aluminides coatings produced on pure Ti by laser surface alloying [J]. Surface & Coatings Technology, 2008, 202: 4121−4129.
[44] BHUSHAN B. Introduction to tribology [M]. New York: John Wiley & Sons, 2002: 210−212.

纯钛表面激光熔覆铁基耐磨涂层结构及摩擦学性能

陈建敏[1]，郭 纯[2]，周健松[1]

1. 中国科学院 兰州化学物理研究所，固体润滑国家重点实验室，兰州 730000；
2. 中国船舶重工集团第七二五研究所，洛阳 471039

摘 要：利用激光熔覆技术在纯钛表面制备铁基涂层。用 XRD、SEM、TEM 分析涂层的相组成和晶体结构。在 UMT−2MT 摩擦磨损试验机上对铁基涂层在不同载荷和不同滑动速度下的摩擦磨损性能进行测试。用 SEM 和 3D 表面轮廓仪分析铁基涂层磨损后的表面形貌和磨屑形貌。结果表明：钛表面激光熔覆制备的铁基涂层的显微硬度约为 860 $HV_{0.2}$，具有优异的耐磨性能，磨损率为$(0.70\sim2.32)\times10^{-6}$ $mm^3/(N\cdot m)$，可以显著提高纯钛基材的耐磨性能；涂层的磨损机理为轻微的磨粒磨损和粘着磨损。

关键词：钛；铁基涂层；激光熔覆；摩擦磨损

(Edited by YANG Hua)